Dynamically Stabilized Pores in Bilayer Membranes

J. David Moroz and Philip Nelson
Department of Physics and Astronomy, University of Pennsylvania, Philadelphia, Pennsylvania 19104 USA

ABSTRACT Zhelev and Needham have recently created large, quasistable pores in artificial lipid bilayer vesicles. Initially created by electroporation, the pores remain open for up to several seconds before quickly snapping shut. This result is surprising, in light of the large line tension for holes in bilayer membranes and the rapid time scale for closure of large pores. We show how pores can be dynamically stabilized via a new feedback mechanism. We also explain quantitatively the observed sudden pore closure as a tangent bifurcation. Finally, we show how Zhelev and Needham's experiment can be used to measure accurately the pore line tension, an important material parameter. For their stearoyloleoylphosphatidylcholine/cholesterol mixture we obtain a line tension of 2.6×10^{-6} dyn.

INTRODUCTION

Lipid bilayer membranes have remarkable physical properties. One of the most important among these properties is a membrane's resistance to rupture. In the body, this resistance is critical to the maintenance of well-defined and properly functioning cells. Indeed, when a cell needs to undergo a topological change (as it does during cell division, cell fusion, endocytosis, and exocytosis), it usually has to make use of specialized machinery that carries out the change at the cost of chemical energy. This cost is largely determined by the material properties of the lipid membranes in question.

We can quantify a membrane's resistance to rupture in terms of a line tension (γ), the free energy cost per unit length of exposed edge. Edges are disfavored because of the high cost of either exposing the hydrophobic lipid chains to water or creating a highly curved rolled edge to hide them. Many authors have devised ingenious indirect measurements of γ in various lipid systems (Taupin et al., 1975; Harbich and Helfrich, 1979; Chernomordik et al., 1985), but direct measurement has proved difficult. Among the biologically relevant questions that require such measurements is the variation of γ with lipid shape (Leikin et al., 1987).

Recently Zhelev and Needham have found a new technique allowing direct mechanical measurement of the line energy (Zhelev and Needham, 1993; Zhelev and Needham, 1994). In this paper we will present a new analysis of their experimental data. The experiment revealed some surprising qualitative phenomena involving pores, which we will explain. Briefly (see below), they created long-lived quasistable pores ~ 1 μm in radius. After persisting for up to several seconds, the pores snapped shut in just one video frame. We will quantitatively explain the longevity of the pores and their sudden demise, fitting several quite different events with a common value of γ and two auxiliary parameters.

To see why long-lived pores are surprising, consider the usual energy of a circular hole in a flat bilayer membrane (Taupin et al., 1975). This energy can be written as a line tension term, which is linear in the pore radius, minus a surface tension term, which is quadratic. The energy thus has the form

$$E(r) = 2\pi r\gamma - \Sigma\pi r^2, \qquad (1)$$

which has only one stable minimum (at $r = 0$). There is a critical radius ($r = \gamma/\Sigma$) above which the pore is unstable to rupture. To cross this critical point, the system must surmount a significant energy barrier ($\Delta E = \pi\gamma^2/\Sigma$). For typical estimates of the line tension (10^{-6} dyn), thermally driven rupture thus requires a surface tension on the order of 1 dyn/cm, as observed (Evans and Rawicz, 1990). For lower tensions, any transient pore will reclose rapidly, whereas for larger tensions it will grow rapidly and lyse the vesicle; in either case, one does not expect large, stable pores to exist.

Nevertheless, Zhelev and Needham found that pores with a radius of ~ 1 μm can remain open and stable for several seconds. In these experiments, giant vesicles are aspirated into the mouth of a micropipette, where they are held in place by suction. A brief electrical field impulse is applied across the vesicle by a pair of capacitor plates. As a result of this impulse, lipid molecules in the membrane rearrange around a newly formed pore through a process known as *electroporation* (Chang et al., 1992).

As noted above, the appearance of large, stable pores is surprising, and yet Zhelev and Needham documented over a dozen such events. They proposed that somehow these events managed to sit on the unstable equilibrium point of Eq. 1 for a long time before suddenly falling off. Inferring Σ and r from the data, they then found the line tension from $\gamma = \Sigma r$. It seems unlikely, however, that the membrane would remain in unstable equilibrium for so long.

In this paper we will find a feedback mechanism that dynamically stabilizes pores. The key to the feedback is the

Received for publication 7 October 1996 and in final form 24 January 1997.

Address reprint requests to Dr. J. David Moroz, Department of Physics and Astronomy, University of Pennsylvania, 209 S. 33rd St., Philadelphia, PA 19104. Tel.: 215-898-0555; Fax: 215-898-2010; E-mail: moroz@student.physics.upenn.edu.

0006-3495/97/05/2211/06 $2.00

relationship between the outflow of solution through the pore and the velocity of the vesicle's leading edge as it is aspirated into the pipette. The result is a reduced surface tension, which is a function of both the projected length of membrane in the pipette and the pore radius. This reduced surface tension yields a new effective energy, which exhibits a thermodynamically stable pore at finite radius. The pore exists for some time before suddenly disappearing. From the critical conditions leading to the loss of stability, we will be able to produce estimates of various parameters in the theory; in particular, we will accurately determine the line tension of the bilayer membrane.

THE EXPERIMENT

Fig. 1 defines our notation. In the experiment, lipid bilayer vesicles are prepared from stearoyloleoylphosphatidylcholine (SOPC) with 50 mol% cholesterol (CHOL) at 24°C. The surrounding solvent is about 0.5 M glucose solution, which effectively prohibits permeation of water through the membrane by the osmotic clamp effect. A micropipette is used to immobilize a chosen vesicle using a suction ($-p$). The suction pressure is held constant throughout the experiment at a distant manometer. Initially a small amount of membrane is pulled into the micropipette, leaving a tense spherical outer bulb of radius R_{init}. A square-wave electric field pulse is then applied across the vesicle; typical pulses produce a field on the order of 100 kV/m for a duration of about 150 μs. The effect of this field is to rearrange lipid molecules at one of the vesicle's poles so as to open a pore in the membrane. Sometimes no large pore opens; in these cases the suction is stepped up and a second pulse is applied. Other times, the electropore is so large that the whole vesicle is sucked rapidly through the micropipette and disappears. But occasionally the pore stabilizes and the vesicle moves slowly down the pipette in a controlled fashion. (Optical contrast methods make visible the jet emerging from the pore, and assure us that the pore does close, rather than just being pulled into the micropipette (Zhelev and Needham, 1993).)

What is measured then is the constant applied suction ($-p$) at the manometer, the initial bulb size (R_{init}), the micropipette diameter (d_p), and the location ($L(t)$) of the leading edge of the membrane as it advances down the micropipette. Fig. 2 shows a typical time course. Other quantities in Fig. 1, such as the bulb radius (R), the pore radius (r), the lubrication layer thickness (h), the surface tensions (Σ, Σ_0), and the pressures ($-p_1$, p_2) are all time dependent and must be inferred from the directly measured data.

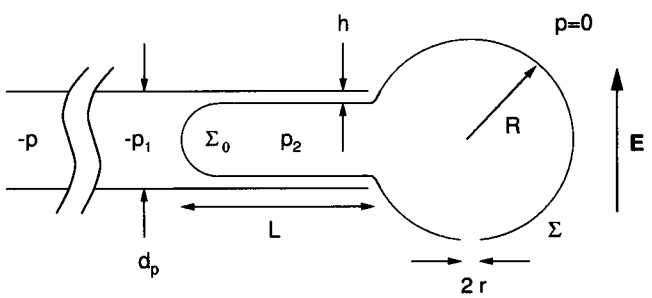

FIGURE 1 Geometry of the stabilized pore experiment of Needham and Zhelev.

As the vesicle moves into the pipette, the suction immediately in front of it is reduced because of Poiseuille loss along the micropipette. The corrected pressure is given by $-p_1$:

$$-p_1 = -p + \frac{32\eta}{d_p^2}(L_{eff} - L)v. \qquad (2)$$

Here η is the viscosity of the sugar solution, L is the projected length of membrane in the micropipette (Fig. 1), and $v \equiv \dot{L}$ is the velocity of the vesicle's leading edge. Equation 2 should really be regarded as a definition of the effective length (L_{eff}), because the micropipette is not really a perfect cylinder of constant diameter. Zhelev and Needham estimated this parameter as 922 μm by noting the velocity at which small beads moved down the tube under similar applied pressures. Given the significant difference between this experiment and the one in question, we will treat L_{eff} as an undetermined experimental parameter of fixed value. (L_{eff} also includes any other constant friction, for example, membrane drag around the lip of the micropipette.) As we shall see later, L_{eff} can be determined from the data of Fig. 2 by using our theoretical approach.

There is a second velocity-dependent friction term that enters into the equation of motion for the vesicle's leading edge. This term is due to shear in the lubricating layer sandwiched between the membrane and the micropipette wall. This frictional force creates a difference between the surface tension (Σ_0) at the leading edge and (Σ) on the

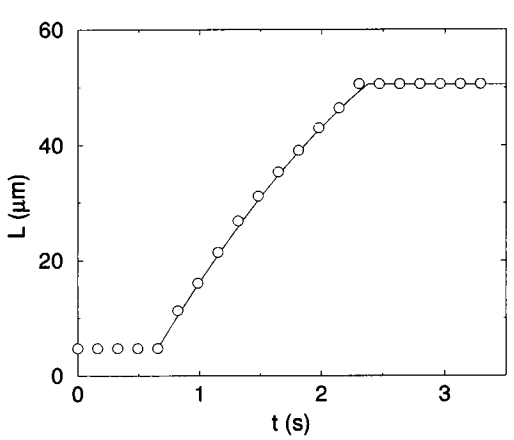

FIGURE 2 Progress of the leading edge of a SOPC/CHOL mixed lipid vesicle down the pipette (reproduced from figure 3 of Zhelev and Needham, 1993). For this event R_{init} = 17.6 μm and p = 353 dyn/cm^2. The initial velocity (v_{init}) is approximately 35 μm/s. The solid line depicts the theoretical $L(t)$ curve for our stabilized pore model.

exterior bulb:

$$\Sigma = \Sigma_0 - \frac{\eta L}{h} v. \tag{3}$$

Here h defines the thickness of the lubrication layer. (In reality, this parameter will be a function of distance along the micropipette and of the projected length itself (R. Bruinsma, preprint 1996). It turns out, however, that the final results are not strongly dependent on h, and so we will treat it as a constant.) An experimental determination of this parameter is somewhat difficult; Zhelev and Needham estimate it to be on the order of 0.2–0.3 μm. As with L_{eff}, we will determine this difficult to measure parameter directly from the data in Fig. 2; our value agrees well with the experimental estimate.

These two sources of friction control the speed of the vesicle front. As we will show in the following sections, they also determine the stable pore size and when and if the pore recloses so as to stop the inhalation process. As the projected length of membrane inside the micropipette grows, so does the amount of friction. We will identify a feedback mechanism through which the velocity, and hence the surface tension, becomes a function of the pore size. This modifies the effective energy function (Eq. 1) and, in doing so, generates a second stable minimum at a finite pore radius (r_{stable}). At L_{crit} the stable minimum disappears and the pore snaps shut.

STABILIZATION MECHANISM

The feedback mechanism mentioned above requires the surface tension on the exterior bulb to be a function of the projected length of membrane in the pipette and the pore size. The first step is to write this tension in terms of the pressure inside the bulb (p_2) using the Laplace formula:

$$p_2 = \frac{2\Sigma}{R}. \tag{4}$$

Here R is the radius of the bulb. This formula really only applies at equilibrium; fortunately, the membrane's fast relaxation and the fact that R and p_2 change rather slowly imply that the surface is never far from this ideal. (A rough estimate of the relaxation time is given by $\eta_{\text{lipid}} r^2/\gamma \approx 0.01$ s; here $\eta_{\text{lipid}} \approx 1$ erg s/cm^3 is the two-dimensional viscosity of the membrane. The pore size (r) provides a measure of the disrupted area, and the line tension (γ) gives the restoring force.)

The radius of the bulb R is already a simple function of L. The necessary relation is obtained from the constraint of fixed vesicle area. (Strictly speaking, the area is not exactly fixed: thermal fluctuations can always be flattened out by tension to produce a larger projected membrane area. For the tensions appropriate here, the area change will not be more than a few percent (Evans and Rawicz, 1990).) We thus have an equation that determines the bulb radius as a function of projected length (L):

$$4\pi R^2 + \pi d_v L = 4\pi R_{\text{init}}^2. \tag{5}$$

Here R_{init} is the radius of the bulb at the time the pore is created, and $d_v \equiv d_p - h$ gives the diameter of the cylindrical portion of the vesicle inside the pipette. Equation 5 assumes that the bulb region remains spherical and that the area of the leading edge does not change significantly as L increases.

The pressure inside the bulb must still be found in terms of L. This is achieved by considering the interface at the leading edge of the vesicle. Here we can apply Laplace's formula again:

$$p_1 + p_2 = \frac{4\Sigma_0}{d_v}. \tag{6}$$

Implicit in this equation is the assumption that the pressure is uniform everywhere inside the vesicle. There will in fact be a small pressure gradient near the pipette mouth due to convergent flow. This pressure change is on the order of $\eta v/d_v$ and turns out to be negligible. Equations 4 and 6 can now be used to eliminate p_2. In addition, we can use Eq. 3 to remove Σ_0 and Eq. 2 to get rid of p_1. This gives us a new form for the surface tension:

$$\Sigma = \frac{2R}{2R - d_v}\left(\frac{p d_v}{4} - \eta v\left(\frac{8(L_{\text{eff}} - L)d_v}{d_p^2} + \frac{L}{h}\right)\right). \tag{7}$$

This equation for the surface tension now has explicit dependence on the projected membrane length (both through L itself and through the function $R(L)$). The dependence on the pore size enters only implicitly through the velocity.

The goal is now to find a suitable expression for the velocity to substitute into Eq. 7. Following Zhelev and Needham (1993), this can be achieved by considering the flow through the pore. As the vesicle moves into the pipette, its volume changes: solvent must exit through the open pore. We compute the rate of outflow (Q) in two different ways and compare to get v. The first way is to write Q as the derivative of the total vesicle volume (Fig. 1):

$$Q = -\frac{d}{dt}\left(\frac{4\pi}{3}R^3 + \frac{\pi d_v^2 L}{4}\right) = \frac{\pi d_v v}{4}(2R - d_v). \tag{8}$$

Note that we have reexpressed all of the time derivatives in terms of the velocity. The R time derivative was obtained by differentiating the area constraint (Eq. 5):

$$\frac{dR}{dt} = -\frac{v d_v}{8R}. \tag{9}$$

The other expression for the outflow can be found from the pressure forcing the flow. Because the flow is at low Reynolds number, Q is just proportional to the pressure drop

across the pore (Happel and Brenner, 1965):

$$Q = \frac{p_2 r^3}{3\eta}. \tag{10}$$

Equations 8 and 10 can now be combined with Eq. 4 to yield the desired expression for the velocity of the leading edge of the vesicle:

$$v = \frac{8}{3\pi\eta d_v}\frac{\Sigma r^3}{R(2R - d_v)}. \tag{11}$$

This equation can now be substituted back into Eq. 7 to yield the promised form of the surface tension. This form has the surface tension as a function of the projected length (L) and the pore size (r):

$$\Sigma(r, L) = \frac{\alpha_1}{1 + \alpha_2 r^3}, \tag{12}$$

where

$$\alpha_1 \equiv \frac{pd_v}{4}\frac{2R}{2R - d_v},$$

and

$$\alpha_2 \equiv \frac{16}{3\pi(2R - d_v)^2 d_v}\left(\frac{8(L_{eff} - L)d_v}{d_p^2} + \frac{L}{h}\right). \tag{13}$$

These equations define the feedback mechanism through which the effective surface tension is modified by the friction terms outlined in the previous section. The next step is to see how this feedback mechanism accounts for the experimentally observed behavior—that is, to see how it stabilizes pores.

Our main physical hypothesis is now that at each moment the pore adjusts quickly to minimize an effective energy similar to that expressed in Eq. 1, but with the tension replaced by the varying quantity just found (Eq. 12). As long as this effective energy has a nontrivial minimum, the pore size will track it. This gives the pore size, and hence $v \equiv \dot{L}$ via Eq. 11 in terms of L. We can then solve this ordinary differential equation to obtain the time course $L(t)$ and compare to the data in Fig. 2. This program relies on the presence of two different time scales: a slow scale for changes of L and R, and a much faster time scale on which the pore size r adjusts and the membrane tension equilibrates. We are adiabatically eliminating the fast variable to obtain a simple dynamics for the slow one. Thus our effective pore energy depends on L:

$$E_{eff}(r, L) = 2\pi r\gamma - \frac{\pi\alpha_1 r^2}{1 + \alpha_2 r^3}. \tag{14}$$

This new form of the energy can indeed have two minima: the trivial one ($r = 0$) that appeared before, and a new one at a finite pore size, depending on L:

$$\left.\frac{dE_{eff}}{dr}\right|_{r_{stable}} = 0 \rightarrow \gamma = \frac{\alpha_1 r_{stable}}{2}\frac{2 - \alpha_2 r_{stable}^3}{(1 + \alpha_2 r_{stable}^3)^2}. \tag{15}$$

As long as L does not exceed some critical value (L_{crit}), there will be a pore size ($r_{stable}(L)$) that satisfies this equation. When the projected length reaches this critical value, the second stable minimum disappears and the pore collapses (Fig. 3). At this point the second derivative of the energy must also vanish:

$$\left.\frac{d^2E_{eff}}{dr^2}\right|_{r_{stable,crit}} = 0 \rightarrow \frac{1 - 7(\alpha_2 r_{stable}^3)_{crit} + (\alpha_2 r_{stable}^3)_{crit}^2}{(1 + (\alpha_2 r_{stable}^3)_{crit})^3} = 0. \tag{16}$$

The resulting equation is not an equation for the pore size, but rather for the product $\alpha_2 r_{stable}^3$, a pure number. The relevant root of Eq. 16 yields $(\alpha_2 r_{stable}^3)_{crit} \approx 0.146$. This number will be useful in the following section, where we will use the critical condition to determine the three undetermined parameters in the problem: the effective pipette length (L_{eff}), the thickness of the lubrication layer (h), and the line tension (γ) of the membrane.

As promised, we have succeeded in reducing the full dynamics of the problem to only one variable, the projected length (L). This can be seen by substituting the surface tension formulae (Eqs. 12 and 13) along with $R(L)$ (Eq. 5) and the newly determined pore size ($r_{stable}(L)$) into the velocity (Eq. 11):

$$\dot{L} \equiv v(L) = \frac{8}{3\pi\eta}\left(\frac{\alpha_1(L) r_{stable}(L)^3}{1 + \alpha_2(L) r_{stable}(L)^3}\right)\frac{1}{R(L)d_v(2R(L) - d_v)}. \tag{17}$$

This equation for $\dot{L}$ as a function of L can now be integrated to obtain $L(t)$, and then compared directly to the experimental results (Fig. 2).

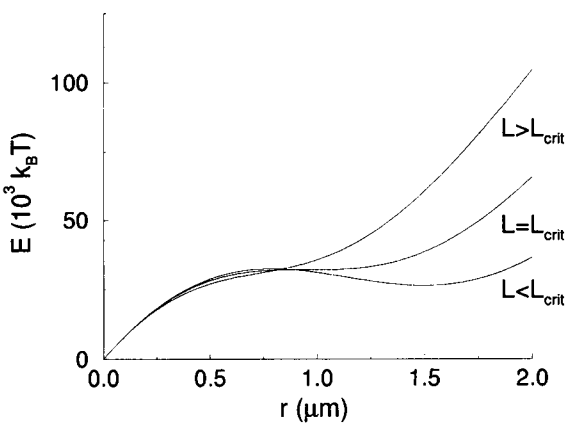

FIGURE 3 Energy as a function of pore size for supercritical, critical, and subcritical lengths of aspirated membrane: L = 0, 45.8, 90 μm (L_{crit} = 45.8 μm).

EXTRACTION OF PARAMETERS

In the last section we were able to find a stable pore size for each value of the projected length of membrane in the pipette. From this pore size we were then able to determine the velocity (Eq. 17). This equation is a first-order nonlinear ordinary differential equation for L. The goal of this section is to fit the unknown parameters γ, L_{eff}, and h so that the solution $L(t)$ fits the event shown in Fig. 2. We will then use these values to explain the other SOPC/CHOL events documented by Zhelev and Needham (1993).

The model that we propose has seven parameters in all (Table 1). Of these, two are measured directly from microscope images, namely the initial bulb radius (R_{init}) and the pipette diameter (d_p). The pressure (p) at the manometer and the viscosity (η) of the solvent are also determined experimentally. (We determined p from Zhelev and Needham (1993): the static tension reported in their table 1 was substituted into their equation 4 to yield the manometer pressure. Zhelev and Needham used different sugar solutions inside and outside the vesicle to get visual contrast. For simplicity, we just used the average of the two measured viscosities in our calculations.)

Of the remaining three parameters, Zhelev and Needham estimated L_{eff} and h via auxiliary experiments, then deduced γ. As discussed in the second section, the effective pipette length was found by using a rather different experiment, and so in our analysis, it will be determined from the data. Our analysis will also yield a value for the lubrication thickness (h) that will be in good agreement with the experimental estimate of Zhelev and Needham (1993). Finally, we will deduce the last remaining parameter in the model: the line tension (γ).

Zhelev and Needham (1993) give the full time course for one event, which we will use to find the three undetermined parameters listed above. This event is reproduced in Fig. 2 and appears as the fourth entry in Table 2 below. From the experimental $L(t)$ curve we first extract the projected length $L_{\text{crit}} = 45.8$ μm at pore closure, the initial velocity $v_{\text{init}} = 35.5$ μm/s, and the final velocity $v_{\text{crit}} = 15.7$ μm/s. We will now use these numbers to determine the three unknown parameters: the effective pipette length (L_{eff}), the lubrication layer thickness (h), and the line tension (γ).

The first step is to require that the pore lose its stability at the observed critical point; the second stable minimum in the energy must therefore disappear at L_{crit}. As noted in the last section, the minimum vanishes when Eqs. 15 and 16 are satisfied. To get the pore size just before closure ($r_{\text{stable,crit}}$) we use Eq. 17 at the critical point and require that it reproduce the observed final velocity. Recalling Eq. 13, we then obtain:

$$v_{\text{crit}} = \left(\frac{(\alpha_2 r^3_{\text{stable}})_{\text{crit}}}{1 + (\alpha_2 r^3_{\text{stable}})_{\text{crit}}}\right)\frac{p d_p^2}{4\eta L_{\text{tot}}}, \tag{18}$$

where we have defined

$$L_{\text{tot}} \equiv 8(L_{\text{eff}} - L_{\text{crit}}) + \frac{d_p^2 L_{\text{crit}}}{d_v h}. \tag{19}$$

Equation 18 can be solved for L_{tot}. Then from Eq. 13 and the value of $(\alpha_2 r^3_{\text{stable}})_{\text{crit}}$, one obtains the critical pore size:

$$r_{\text{stable,crit}} = \left((\alpha_2 r^3_{\text{stable}})_{\text{crit}}\frac{3\pi(2R - d_v)^2 d_p^2}{16 L_{\text{tot}}}\right)^{1/3}. \tag{20}$$

In Eqs. 13 and 20 the value of R is to be taken from Eq. 5 with $L = L_{\text{crit}}$. Using the critical pore size obtained above, we can now go back to Eq. 15 to obtain a numerical estimate for the product of the line tension and a yet to be determined multiplier:

$$\gamma\frac{d_p}{d_v} = \frac{p d_p R}{4}\left(\frac{3\pi d_p^2 (\alpha_2 r^3_{\text{stable}})_{\text{crit}}}{16(2R - d_p)L_{\text{tot}}}\right)^{1/3}\frac{2 - (\alpha_2 r^3_{\text{stable}})_{\text{crit}}}{(1 + (\alpha_2 r^3_{\text{stable}})_{\text{crit}})^2}. \tag{21}$$

On the right-hand side we have made the approximation $(2R - d_v)^{1/3} \approx (2R - d_p)^{1/3}$, which is accurate to within a couple of percent.

The next step is to determine the parameters L_{eff} and h. So far we have found only one combination of these, namely the quantity L_{tot} introduced in Eq. 19. To separate out the two contributions to L_{tot}, we now require that the initial velocity (v_{init}) come out as observed. From the velocity formula (Eq. 11) evaluated at $L = 0$, we can find the effective pipette length in terms of the initial pore size ($r_{\text{stable,init}}$) and the initial velocity:

$$\begin{aligned} L_{\text{eff}}(v_{\text{init}}, r_{\text{stable,init}}) &= \frac{p d_p^2}{32\eta v_{\text{init}}} - \frac{3\pi(2R_{\text{init}} - d_v)^2 d_p^2}{128 r^3_{\text{stable,init}}} \\ &\approx \frac{p d_p^2}{32\eta v_{\text{init}}} - \frac{3\pi(2R_{\text{init}} - d_p)^2 d_p^2}{128 r^3_{\text{stable,init}}}. \end{aligned} \tag{22}$$

TABLE 1 Parameters in the model

Name	Value
R_{init}, p	See Table 2
d_p	7.5 μm
η	0.014 erg s/cm^3
L_{eff}, h, γ	Fixed by model

TABLE 2 Comparison of experimental (Zhelev and Needham, 1993) and theoretical (this paper) closure times for SOPC/CHOL vesicles

R_{init} (μm)	p (dyn/cm^2)	t_{exp} (s)	t_{th} (s)	Bilayers
18.3	399	—*	2.9	1
28.1	310	2.6	3.3	1
14.3	331	—*	—*	1
17.6#	353	1.7	1.7	2
17.0	324	0.33	0.31	2
16.3	337	0.33	0.47	2
16.0	355	2.0	1.0	2
25.6	168	11.0	11.0	1
22.5	240	5.5	5.5	1
16.2	320	2.5	4.6	1

*Did not reseal.
#Event used to determine L_{eff}, h, and γ.

This form for L_{eff} can then be substituted back into Eq. 15 to obtain a sextic equation for $r_{stable,init}$ that can be solved numerically. The solution so obtained can be substituted back into Eq. 22 to yield a numerical estimate of L_{eff}. Finally, the lubrication layer thickness (h) can be recovered using Eq. 19. The approximations considered in Eqs. 21 and 22 can now be refined by using this new value of h through a bootstrapping method.

To finish, we recover the line tension from Eq. 21 by multiplying through by the factor $(1 - h/d_p)$. Thus all three of the required parameters can be determined from the single aspiration event depicted in Fig. 2: $\gamma = 2.6 \times 10^{-6}$ erg/cm, $L_{eff} = 313$ μm, and $h = 0.48$ μm. This value of h agrees with Zhelev and Needham's estimate, whereas our L_{eff} differs considerably from theirs.

With the parameters so determined, it is now possible to determine the time evolution of the other events in Zhelev and Needham (1993) from the initial conditions. For each of the other nine SOPC/CHOL events reproduced in Table 2, we integrated Eq. 17 for the given initial bulb radius (R_{init}) and pressure (p) to obtain the critical time at which the pore closed. In some cases a double bilayer with twice the nominal line tension was needed to fit the data (Zhelev and Needham, 1993). The table compares the experimental time to closure found by Zhelev and Needham to the theoretical time determined using the model. The same effective pipette length, lubrication thickness, and line tension were used for all 10 events. An effort to optimize the values of the three parameters (L_{eff}, γ, and h) based on a least-squares fit to the critical time data did not produce results significantly different from those presented above.

Although the parameters were fixed by data from a single event, they produce reasonable critical times for the entire data set. The first event in Table 2 is clearly an exception that we have no explanation for. Perhaps there was a large fluctuation in the manometer pressure or perhaps the electric field generated a pore so large that relaxation to the stable pore size was impossible. Despite this anomaly, we are confident that we have faithfully determined the line tension of the SOPC/CHOL membrane making up the vesicles in question.

CONCLUSION

In this paper we have explained the existence of the large, dynamically stabilized pores observed by Zhelev and Needham (1993). By separating the fast time scale on which the membrane relaxation occurs from the slow one associated with the motion of the aspirated vesicle down the pipette, we have been able to establish a modified pore energy function with a stable minimum in the 1-μm range. In addition, we have described a new mechanism by which this minimum disappears, destabilizing the pore.

The theory that we have developed permits an accurate determination of an important membrane parameter: the line tension. From a single event in Zhelev and Needham's work, we were able to determine this parameter and two auxiliary parameters. The values so determined were then used to reconstruct all 10 of the published SOPC/CHOL mixed lipid events: our theoretical postprediction for the critical time at which pore stability is lost agreed well with the experimental result for all but one event. The agreement supports the value of our theory as a method for experimentally determining the line tension of bilayer membranes.

We would like to thank R. Kamien, U. Seifert, and D. Zhelev for helpful discussions, and the referee for suggesting an improvement to our calculation.

This work was supported in part by US/Israeli Binational Foundation grant 94-00190 and National Science Foundation grant DMR95-07366. JDM was supported in part by an FCAR Graduate Fellowship from the government of Québec.

REFERENCES

Chang, D., B. Chassy, J. Saunders, and A. Sowers. 1992. Guide to Electroporation and Electrofusion. Academic Press, San Diego, CA.

Chernomordik, L., M. Kozlov, G. Melikyan, I. Abidor, V. Markin, and Y. Chizmadzhev. 1985. The shape of lipid molecules and monolayer membrane fusion. *Biochim. Biophys. Acta.* 812:643–655.

Evans, E., and W. Rawicz. 1990. Entropy-driven tension and bending elasticity in condensed-fluid membranes. *Phys. Rev. Lett.* 64:2094.

Happel, J., and H. Brenner. 1965. Low Reynolds Number Hydrodynamics. Prentice-Hall, Englewood Cliffs, NJ.

Harbich, W., and W. Helfrich. 1979. Alignment and opening of giant lecithin vesicles by electric fields. *Z. Naturforsch.* 34a:1063–1065.

Leikin, S., M. Kozlov, L. Chernomordik, V. Markin, and Y. Chizmadzhev. 1987. Membrane fusion. *J. Theor. Biol.* 129:411–425.

Taupin, C., M. Dvolaitzky, and C. Sauterey. 1975. Osmotic pressure induced pores in phospholipid vesicles. *Biochemistry.* 14:4771–4775.

Zhelev, D., and D. Needham. 1993. Tension-stabilized pores in giant vesicles. *Biochim. Biophys. Acta.* 1147:89–104.

Zhelev, D., and D. Needham. 1994. The influence of electric fields on biological and model membranes. *In* Biological Effects of Electric and Magnetic Fields. D. Carpenter and S. Ayrapetyan, editors. Academic Press, San Diego. 105–142.